A model generating aspects of zebra and other mammalian coat patterns

Article *in* Journal of Theoretical Biology · December 1981

DOI: 10.1016/0022-5193(81)90109-0 · Source: PubMed

1 author:

Jonathan Bard
The University of Edinburgh
193 PUBLICATIONS **10,440** CITATIONS

SEE PROFILE

J. theor. Biol. (1981) **93**, 363–385

A Model for Generating Aspects of Zebra and Other Mammalian Coat Patterns

JONATHAN B. L. BARD

MRC Clinical and Population Cytogenetics Unit, Western General Hospital, Crewe Road, Edinburgh EH4 2XU, Scotland

(*Received* 9 *January* 1981, *and in revised form* 8 *April* 1981)

A model is put forward which is capable of generating chemical maps whose concentration contours are similar to the patterns seen on the flanks of zebras, cats and other mammals. The model derives from the reaction–diffusion kinetics invented by Turing (1952) and it is assumed that the necessary molecular apparatus is present in each cell of a two-dimensional array and that the cells are in diffusion contact. The model was expressed in differential equation form and solved digitally under a range of different initial, boundary and other conditions. The main forms of pattern that the model generated were spots of variable complexity, rings, and both vertical and horizontal stripes. If morphogen concentration levels are assumed to act as melanin-production switches, then a common basic mechanism is capable of generating a variety of skin patterns. Simple spots such as those found in the fallow deer or the serval, *F. serval*, are generated if the kinetics are initiated simultaneously in each cell and interpretation depends only on the presence or absence of morphogen, which is assumed for the deer to be an activator and for the cat a suppressor of pigment formation. The reticulated pattern of the giraffe is generated if there is a single high-value threshold. Complex spots typical of the leopards can be produced if there are different concentration thresholds for different colours. Rings of pattern typical of those found on cat tails are generated if the cellular array is a very narrow cylinder. Horizontal stripes are generated if the kinetics in each cell are initiated by a diffusion gradient whose source is the dorsal line of cells and these stripes may break up into spots to give a pattern very similar to that of, for example, the fishing cat, *F. viverina*. The vertical stripes of the caffre cat, *F. caffra*, or the zebras are formed if the kinetics are initiated by a vertically-moving constant-velocity wave which also allows morphogen diffusion between previously uncoupled cells. Thus far, the mechanism has generated neither the triradii that are commonly found on forelimbs nor the rings often observed on mammalian limbs. It does however incorporate the randomness that characterizes skin pattern, its operation is of the scale required in embryogenesis, it can be made stable to growth and it can explain certain degenerate patterns. Analysis of a spotted zebra in the light of the model provides evidence that zebra stripes arise from the inhibition rather than the stimulation of melanin; their pattern is thus of white stripes on a black background.

0022-5193/81/220363 + 23 $02.00/0

Introduction

The many, instantly recognizable patterns in the pigmentation of the hairs in the mammalia comprise a complex range of stripes and spots. In general, virtually nothing is known of the mechanisms by which they are laid down or even what the relationship is between the patterns in closely-related species. There is however some evidence on when the pattern of zebra stripes is determined: analysis of the growth of the *equidae* suggests that pigmentation decisions take place at around 3–5 weeks of development even though the hairs that show the pattern do not grow until about 6 months (Bard, 1977). One compensating simplicity that does emerge from this analysis is that, although adult zebra pattern may show body stripes of many widths and orientations, it is likely that the pattern when first laid down is of evenly-spaced, dorso-ventral stripes and it is differential growth that is responsible for the complexity of the adult pattern (Fig. 1). If this analysis is correct and can be generalized, it does at least mean that pattern formation in the mammalia reduces to generating a uniform array of elements.

The possible mechanisms that are known to be capable of giving rise to coat patterns are relatively few in number. Simple uneven blotches of colour with perhaps several repeats can be generated by clonal growth (Mintz, 1971; Wolpert & Gingell, 1970) while spots or a single horizontal body stripe can arise from the migration of melanoblasts under the constraints of a variable amount of negative chemotaxis (Twitty, 1945). Many patterns in embryos can be set up by gradients; cells may interpret gradient values through thresholds (Wolpert, 1969), but only with highly sophisticated and complex interpreting mechanisms (e.g. MacWilliams & Papageorgiou, 1978) can they be interpreted to give the repeating patterns of mammalian skin markings. In principle, the most powerful mechanism for forming such patterns is based on reaction-diffusion kinetics which were invented by Turing (1952). These generate concentration peaks and troughs over cellular arrays and have a natural repeating distance, the chemical wavelength. Searle (1968) has pointed out that were such a chemical pattern to exist in epidermis it could readily be interpreted through simple thresholds to initiate a similar pattern of melanin production. More recently, Murray (1981) has shown analytically that reaction–diffusion kinetics are capable of generating concentration maps that mimic several features of coat patterns.

In this paper, I examine in detail one set of kinetics invented by Turing (1952) and explore the range of patterns it can generate under a variety of different conditions and when modified in several ways. In particular I

study the role of thresholds and initiating conditions and touch on the role of boundary conditions. I show that there is great similarity between the theoretical patterns and those observed on the flanks of certain mammals, mainly cats and zebras. This paper concentrates on the flank in particular as its geometry is simple; in consequence shape constraints probably play only a minor role in determining pattern. The discussion examines, in the main, the extent to which morphological similarity between theoretical and natural patterns gives grounds for supposing that the model reflects biological reality.

A Note on Zebra and Cat Patterns

The most noticeable feature of various species of zebra is the large number of dorso-ventral (D-V) body stripes of variable width. In addition, they all have a triradial stripe on the forelimb which marks the position distal to which the pattern becomes circular rings around the limbs. In *E. grevyi*, the imperial zebra, there is a triradius on the hind leg and a dorsal stripe over the back. In *E. burchelli*, the common zebra, there is also a dorsal stripe but the hind quarters have a few broad caudal stripes and shadow stripes between them (Fig. 1). In *E. zebra*, the mountain zebra, there is no dorsal stripe but there are three caudal stripes (see Bard, 1977,

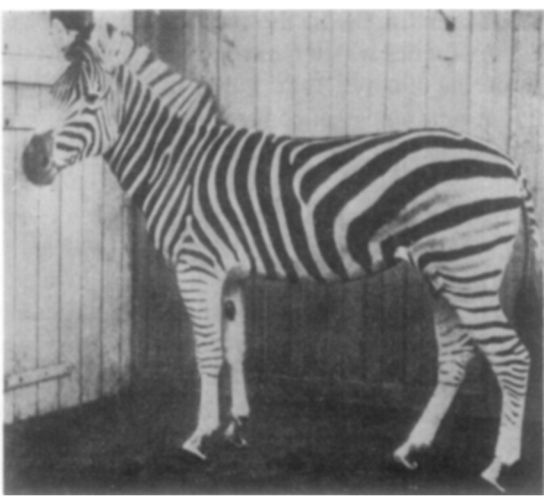

FIG. 1. *E. burchelli*, the common zebra, shows a range of pattern elements: these include dorsal, vertical and caudal stripes, a triradius on the forelimb and rings around the limbs and ear. Between the broad caudal stripes that extend from the belly to the rump are intervening grey shadow stripes.

for more details). The quagga, *E. quagga*, has the striping of *E. burchelli* at the front and a simple black hindquarter (Rau, 1974). In all cases the body and head stripes were, when first laid down, in the embryo, probably regularly spaced being about 0·4 mm wide and 0·5–1·0 mm long. Cat patterns are far more varied and variable (Lynnender, 1900) and a member of the *felidae* may have pattern elements drawn from a range that includes one or more dorsal stripes, anterior–posterior (A-P) and/or D-V stripes, spots of various degrees of complexity, triradii and rings or stripes which sometimes appear to break up into spots. In the domestic cat, there may also be large patches of colour with irregular edges. These will be assumed to derive from clonal growth and will not be considered further here. There is one additional feature that marks all mammalian skin patterns: although there are great similarities among animals within a species, no two animals are ever identical, indeed there are differences between the two flanks of a single animal. With one or two notable exceptions (see end of discussion) other mammalian patterns can be viewed, formally at least, as similar to those of the cats.

The Model

The model discussed here contains various constituent elements, the most important and central of which is the chemical network supposed to exist in each cell that partakes in the pattern-forming process. This network generates the kinetics which control morphogen production. It is the peculiar nature of the kinetics that, when morphogens diffuse between cells, small random differences in concentration are amplified via positive feedback controls to cause a concentration distribution that is, initially, roughly uniform across a tissue to break up and give a chemical pattern with a characteristic wavelength. There are however other important features to the model: these include the way in which the kinetics are initiated and interpreted, the form and size of the array over which the kinetics operate and certain modifications to the basic chemical mechanism. It is the purpose of this section to describe these various facets and, as the model itself was written as a lengthy computer programme, it ends with a brief enumeration of the important variables and options that specified any simulation of a pattern-formation process.

TURING KINETICS AND MODIFICATIONS

Turing wished to show that organization could emerge in a bland embryo of identical cells which could only synthesize or break-down molecules and

which were in diffusion contact with neighbours. He therefore invented theoretical chemical networks now known as reaction–diffusion processes which are capable of generating spatial patterns of chemical concentrations. He demonstrated (1952) that, under highly restricted conditions, two interrelated molecules (whose names and concentrations are designated X and Y) could form a stable inhomogeneous concentration map and could act as morphogens. The energy required to maintain the pattern against the normal dissipating effects of diffusion comes from a continuous flux of source molecules to morphogens to breakdown products, and the pattern disappears once the source molecules are exhausted. The detailed theory was given by Turing (1952) and a simple formulation of one set of the kinetics by Bard & Lauder (1974). It is the latter version that will be given here in summary and the interested reader is referred to the literature for details.

The chemical network for the two morphogens X and Y is complicated, but the kinetics themselves can be described by a pair of relatively simple differential equations that each contains two terms, the first describes the synthesis of a morphogen, the second its diffusion among neighbours. For a cell with two neighbours, say the rth cell in a line, the equations are:

$$\frac{dX_r}{dt} = \frac{S}{16}(16 - X_r Y_r) + \mu(X_{r+1} - 2X_r + X_{r-1})$$

$$\frac{dY_r}{dt} = \frac{S}{16}(X_r Y_r - Y_r - \beta_r) + \nu(y_{r+1} - 2y_r + y_{r-1}).$$

In general, the diffusion terms depend on the number of neighbours with which a particular cell is in contact. In the equations, S is a constant whose size controls the spacing of the pattern (between three and 50 cells), μ and ν are diffusion constants and β_r is the concentration of a particular enzyme in the rth cell. This last factor is uniquely important for, if each cell has identical kinetics and initial concentrations, then it is clear that the diffusion terms will always be zero, each cell will in effect be autonomous and no pattern will form. In practice, of course, cells are never identical and natural variation is built into the system by making the amount of the enzyme β unpredictable. Its value is set from a normal distribution of mean 12·0 and a discretional standard deviation through a random number generator. The presence of β acts as a pattern-formation switch: there is a normal stable equilibrium of $X = 1$, $Y = 16$ when $\beta = 0$ and an unstable equilibrium of $X = Y = 4$ that breaks up to give a repeating pattern when $\beta = 12 \pm \sigma$ ($\sigma \geqslant 0{\cdot}005$). It turns out to be a feature of this pattern that Y has a maximum value of about 6·0 concentration units and a minimum value of

0·0 while X has a maximum value of about 7·5 and a minimum value of about 3·0, the two patterns being exactly out of phase. When, in the units of the system (see below), $S = 1{\cdot}0$, $\mu = 0{\cdot}25$ and $\nu = 0{\cdot}0625$, the wavelength for a linear array is about seven cells.

As the equations stand, there is no reason why a cell which has no Y at some time should maintain this state if the conditions alter. In order to stabilise patterns on growing arrays a "zero-fix" threshold condition has been introduced: this ensures that, once a cell has reached zero concentration for Y, it maintains that state indefinitely. In computing terms, this is a simple instruction; a possible molecule mechanism is that Y inhibits the production of a non-diffusible enzyme that devours Y voraciously. In the absence of Y, this enzyme is synthesized and then ensures that any Y that ever reaches that cell is broken down immediately.

There is a further instruction in the programme which merits explanation. This instruction ensures that Y cannot become negative. The equations as they stand do not forbid this due to an oversimplification in the β term. The exact term for the degradation of Y by β is $K.\beta.S.Y./(K_m + Y)$ where $K = 62{\cdot}5$, $\beta = (12 \pm \sigma) \times 10^{-3}$ and K_m is very small (Turing, 1952; Bard & Lauder, 1974). Provided $Y > 10^{-2}$, β is saturated and the degradation term reduces to $S(12 \pm \sigma)/16$. When Y is very small, the exact term should be used and this of course tends to zero with Y. In order to keep the program as short as possible, the exact dynamic was abbreviated. The approximation is only invalid at very low values of Y and its effect is only to slow slightly the time taken for the concentration of Y to reach zero in that cell.

THE CELLULAR ARRAYS

Three arrangements of cells were used: rectangles, cylinders and cones. Rectangles and cylinders differ formally only in their boundary conditions: rectangles have non-leaky edges while the cylinder is a rectangle folded so that one pair of opposite sides are in diffusion contact. A cone was modelled as a series of wrapped rectangles of successively smaller width (see Fig. 6). In most cases, cells were assumed rectangular, having in general four nearest neighbours. Hexagonal and diamond arrays were also used but, as the patterns that emerged for a given set of conditions turned out to be independent of the local cellular organization, these will not be mentioned further.

UNITS

For a reasonable biological simulation, convenient units are the second for time and a length of 10 μm for distance, this being the value set for a

cell diameter. In these units, diffusion constants are 10^6 those in cgs units and the values of 0·25 and 0·0625 correspond to cgs values of 2·5 and $0{\cdot}625 \times 10^{-7}$. In fact, the unit of distance is not of major importance as the formulation of the kinetics assumes that diffusion is membrane-limited. The results are thus in units of cell number. Concentration is in arbitrary units.

It turns out that to obtain a given pattern, the computing time varies at the fourth power of the wavelength. In order to keep the computing within reasonable bounds, a chemical wavelength of about 9 cells was taken and this results from choosing a kinetic speed value (S) of 0·5. The fastest iteration value possible was 0·85 sec and the "real" time taken for a large array where all cells were initiated simultaneously to reach a chemical equilibrium was about 1200 sec. If that array was 20×20 cells, computing time on an IBM 370 computer was about 5 min.

PATTERN INITIATION

It turns out that the pattern generated by the kinetics depends on how they are initiated as well as on the biochemical details. The pattern formation process starts when the enzyme β is made available to degrade the morphogen Y in a cell and, in the simplest of cases, this occurs in all cells in the array simultaneously. Prior to this, the kinetics were at the "$\beta = 0$" equilibrium where $X = 1$ and $Y = 16$. Two other modes of initiation have been investigated, one depending on diffusion, the other on a constant-velocity wave. The first assumes that the dorsal line of cells synthesizes at a constant rate a diffusible initiator Z that moves ventrally inducing β in any cell in which the concentration of Z exceeds some threshold. In these simulations, the source concentration of Z was held at 10·0, its diffusion constant 0·05, the threshold value 2·0 and all cells were assumed to be in diffusion contact whether or not the threshold had been exceeded. For the last option, initiation was achieved by a constant-velocity activating wave moving dorsally from the ventral line of cells. In these simulations the cells were initially set to be isolated so that the morphogens X and Y could not diffuse between them. A line of cells was activated when the wavefront reached it and this activation not only started β production but also permitted diffusion to occur betwen cells previously activated and the new line. In computing terms, this mode is easy to set up as, after a fixed increment of time, a new line of cells is activated. At the biological level, a mechanism for a constant velocity wave has been put forward by Britton & Murray (1979). The simple activating mechanism assumes a uniform array, the other two give this array a dorsal–ventral polarity.

INTERPRETATION OF THE PATTERN

The computer simulation eventually gives the equilibrium values of morphogen concentration in each cell. The simplest way of translating this chemical pattern to a pigment pattern is to identify those cells where the Y concentration drops to zero and assume that the presence or absence of the morphogen acts as a switch. Such cells will in general be shown in the figures as black and referred to as "zeros". In general, however, one must assume that the chemical pattern is transformed to a differentiation pattern via a threshold-interpretation system where the threshold may have an arbitrary value (see, in particular, Fig. 2). Lewis, Slack & Wolpert (1977) have put forward a mechanism by which this can be done if several levels are required. Here, a mechanism is taken for granted and only concentration contours are used.

THE COMPUTER PROGRAM

The model was expressed as a computer program in FORTRAN and run on an IBM 370 computer (see Bard & Cauder (1974) for details). The options required for a given simulation were as follows.

(1) *The kinetics*

(i) Speed (S): fixes the chemical wavelength
(ii) standard deviation of $\beta(\sigma)$
(iii) A random number generator: seed number (N)

(ii) and (iii): together, these determine the amount of the enzyme β in each cell.

(iv) Zero-fix option: Whether a cell that once has a zero concentration of Y should maintain this value.

(v) Stability constant (E): the simulation ends when the ratio of the change in concentration to the absolute concentration in all cells is less than the stability constant for three successive iterations. A typical value would be 10^{-3} and measures the closeness to equilibrium approached by the kinetics.

(2) *The array*

(i) Size and shape: rectangle, cylinder, or cone.
(ii) Cell organization: rectangular, hexagonal or diamond shaped.

(3) *Mode of initiation*

(i) Simultaneously in all cells.
(ii) Diffusion activation in a D–V direction.
(iii) Constant velocity wave of activation in a D–V direction.

The output from the computer generated the concentrations in each cell at suitable time intervals, the appropriate cellular organization being programmed so that the emerging pattern was easy to see on the printout.

Results

The basic pattern that forms when Turing kinetics operate over a two-dimensional cellular array is of concentration peaks and troughs. The chemical contour map of the Y morphogen shows a roughly uniform concentration value of about 6·0 units punctuated by dips where the concentration drops to zero. The X morphogen has a low baseline value of about 3·0 concentration units that rises to peaks of about 7·0 units at the points where the Y morphogen dips. The major factor that was found to alter this basic pattern was the mode of initiation, a further influence was the presence of circular boundary conditions; the results are grouped accordingly. The basis of the computing simulations are given in the text, but the details for a given pattern are relegated to figure legends. The general outline of each part of this section is first to describe the patterns that form under one or another mode of initiation, then to consider the reasons why the patterns emerge and finally to compare them with similar patterns on animal coats. For this, the position of zeros of the Y morphogen will in general be used to give the pattern elements as this mode of interpretation provides the simplest switching system for melanin production. The role of the other morphogen and thresholds in modulating these basic patterns will also be considered. In all of this analysis, it is usually assumed that once a cell is determined to provide pigment, this decision is irreversible not only for the cell but also for its progeny (zero-fix option).

UNIFORM ACTIVATION OVER A RECTANGULAR ARRAY

As mentioned, this simplest mode of initiating the kinetics gives rise to two superimposed groups of spots with a characteristic pattern but of irregular and unpredictable position (Fig. 2a). The boundaries of the array encourage the formation of local zeros (see also Fig. 7); but, as such boundaries do not exist in the skin, these zeros are of no biological significance. The time taken for the pattern to stabilize over a two-dimensional array is independent of array size as diffusion is relatively local and, for a speed value of 0·5 and a stability criterion of 10^{-4}, is about 20 min. The physico-chemical reasons why the pattern of spots should form are complex and derive from the autocatalytic aspects of the kinetics which are amplified by diffusion. Here, we shall take this basic pattern of spots

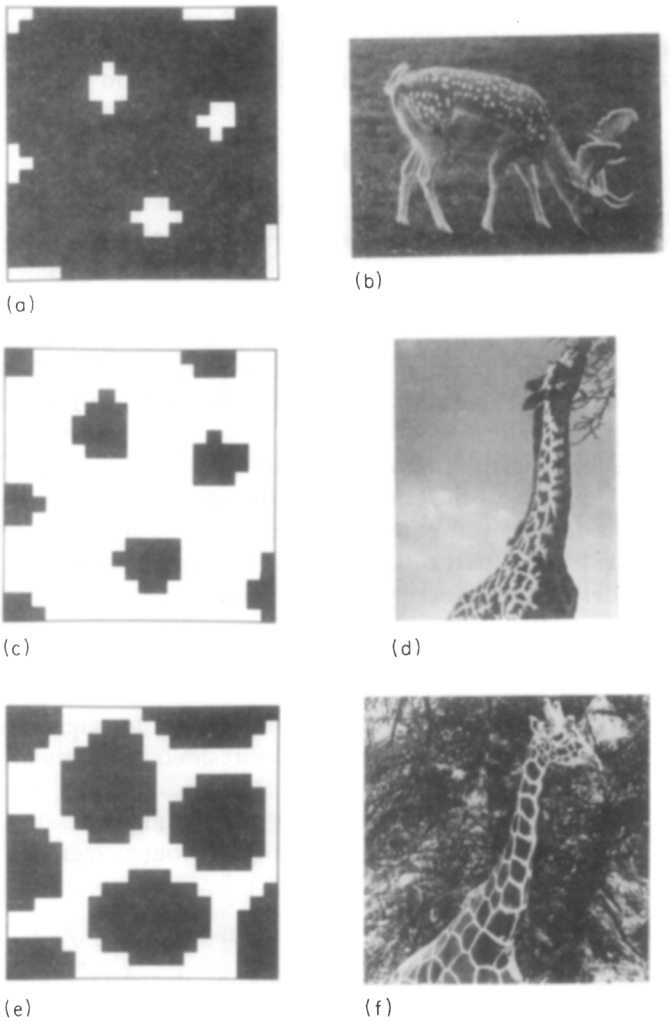

FIG. 2(a) A Turing pattern of the Y morphogen on a 20×20 array of cells after 20 min. In this pattern, the zeros are shown as white on a dark background; in pattern terms, this corresponds to the Y morphogen acting as a pigment initiator. Computing details: $S = 0{\cdot}5$, $\sigma = 0{\cdot}25$, $N = 91563$, $E = 10^{-4}$. (b) The fallow deer: the flank pattern of this animal is of small white spots of on a dark background. (c) The same simulation shown in Fig. 2a. In this case, however, the X morphogen is shown and the black areas mark those cells where the concentration exceeds a threshold of 5·0. (d) A Masai giraffe: its pattern is of large irregular dark patches on a light background. (e) The simulation shown in Fig. 2a. Here, the cells that have an X morphogen concentration greater than a threshold value of 3·4 are marked. (f) A Cape giraffe: its pattern is reticulated appearing as large dark blocks separated by thin light lines.

for granted and only consider how it can be modulated and refer the interested reader to Turing's original paper for a detailed explanation.

The way in which a chemical pattern of spots would make itself manifest in the embryo depends entirely on the mode of interpretation of morphogen concentration. The simplest mechanism might occur if, say, Y is a melanin activator; in this case the pattern would be of white spots on a dark background (Fig. 2a)—the pattern of the fallow deer (Fig. 2b). If, on the other hand, Y were a melanin suppressor, the expected pattern would be black spots on a light background—the pattern of the cheetah. Such sharp light–dark spotted patterns are however rare; far more common is a two-tone pattern based on a single colour. The most obvious explanation of these in the morphogen context is to assume that there are concentration thresholds in each cell above or below which it produced pigment in either different amounts or in different colours. Dark spots on a light background are found in the cats, notably in the leopards and the serval (see Fig. 6). The few stripes around the tail will be considered later.

Changing threshold values can cause the pattern to take up different aspects. There are, for example, two species of giraffe: the Masai variety has large spots (Fig. 2d) while the Cape giraffe has a reticulated pattern of large dark regions separated by thin white lines (Fig. 2f). These differences can be explained by suggesting that the interpretation threshold of the X morphogen is different in the two species (see Figs 2c and e and corresponding legends). More complex patterns can be built up if there is more than one threshold or if each morphogen is able to elicit a different colour. The clouded leopard, for example, has a beige background on which are large spots with a dark periphery and a light centre. A mechanism by which the threshold would have to be interpreted in order that the darkest colour arises at an intermediate concentration value is unlikely to be simple. Possible ways of generating such patterns for the concentration map include complex thresholds (Lewis *et al.*, 1977; MacWilliams & Papageorgiou, 1978) and cascade processes whereby the first set of kinetics stimulates a second set over a domain defined by the contours.

ACTIVATION WITH A DIFFUSION GRADIENT

For these simulations, an array of equivalent, initially-unpolarised cells have, at the top or dorsal edge, a line of cells that synthesizes an activator that diffuses ventrally and initiates the kinetics in a cell once its concentration there exceeds some threshold. Under these conditions, the pattern that forms initially is A–P lines of zeros. The number of these lines depends on the variation in the amount of the enzyme β among the cells: if the

standard deviation is low, ~0·05, there are five or more lines (Fig. 3a), if the standard deviation is higher, two or three lines form and, ventral to these, are rows of spots (Fig. 3b). The physical basis of this pattern probably derives from the way that diffusion gradients are set up in the array and from the consequent local diffusion of the morphogens. Consider the activation over the first few lines of cells: as diffusion is initially very fast these cells are activated almost simultaneously. As there will be much larger differences between activated and non-activated cells than between adjacent activated cells, there will be far more diffusion in the D–V than in the A–P directions. The effect of this is that, to a first approximation, there will be higher diffusion fluxes between D–V than between A–P neighbours. This in turn means that the system behaves as similar D–V

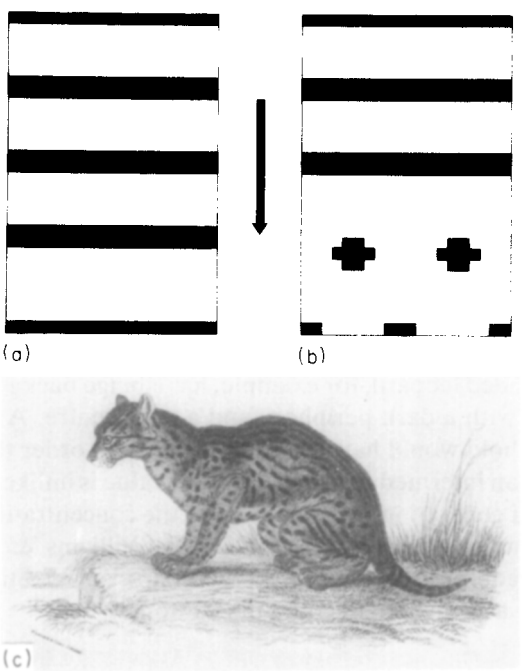

FIG. 3(a) The pattern of Y morphogen zeros that emerged over a 30×20 array of cells when initiated by an activator diffusing ventrally (arrow). Computing details: $S = 0{\cdot}5$, $N = 84643$, $\sigma = 0{\cdot}05$. Cells were activated when the concentration of the activator, whose diffusion constant was 0·05 and whose dorsal value was maintained at 10·0 units, exceeded a threshold of 2·0. The pattern took about 2 hr to form. (b) A simulation identical to that of Fig. 3a except that the standard deviation (σ) of the β enzyme was 0·1. (c) The fishing cat, *F. viverrina*, has a pattern of dorsal stripes that breaks up ventrally into spots. In order to identify this pattern with that of Fig. 3b, it is necessary to assume that the flank lengthened after pattern formation and so stretched out the spots there (from Lynnender, 1900).

columns of cells. The polarity imposed by the most dorsal cell being activated first causes a zero to form there and, after that, each column behaves similarly forming contiguous spots that together appear as a line. Once the first few rows of zeros have formed, the rate of cell activation declines markedly, gradients are less as diffusion occurs between activated and non-activated cells and consequently the amounts of D–V diffusion relative to that in the A–P direction declines. At this point, cells become more influenced by the A–P neighbours and there begin to be "row" effects; these cause the line of zeros to break up into spots. The number of unbroken rows of zeros thus depends on the standard deviation of β: if it is low, columns remain isolated longer and more rows form; if high, there are fewer complete rows of zeros. It is important to note that this pattern is stable whether or not the zero-fix option is used. A–P lines of pigment are mainly seen in the cats: a particularly good example of a mammal with dorsal lines of pigment and ventral rows of spots is the fishing cat, *F. viverrina* (Fig. 3c).

ACTIVATION WITH A CONSTANT VELOCITY WAVEFRONT

A third way of initiating the kinetics is with an activator of the Turing kinetics which moves ventrally through the array at constant velocity. This contrasts with diffusion where the velocity is position-dependent. Constant velocity waves moving through tissues have not been explored in detail, but Britton & Murray (1979) have provided a theoretical molecular mechanism for the phenomenon. I shall not consider the mechanism details here but merely assume that a *slow* wave of activation moves through the tissue initiating successive cells down the array at fixed time intervals. The significance of "slow" in this context is that the kinetics in a cell approach equilibrium before the cell ventral to it is activated. In practice this means a time interval of 5 min between successive line activations. For these simulations, activated cells are chemically isolated from non-activated cells and, in a sense, this system is formally equivalent to growth where the distal line of cells is undergoing mitosis.

Using standard kinetics and the zero-fix condition, the pattern that arose was of a series of D–V stripes whose spacing was that of the chemical wavelength (Fig. 4a). If the zeros were not fixed, the pattern would readily break up into spots unless the standard deviation in β was very low; when the zeros were fixed the pattern was stable. The behaviour of the dorsal line of cells in the array was found to depend on how long the initial cells were activated before successive ones. Using the standard 300 sec increment, a top horizontal stripe and a row of spots emerged before the stripes.

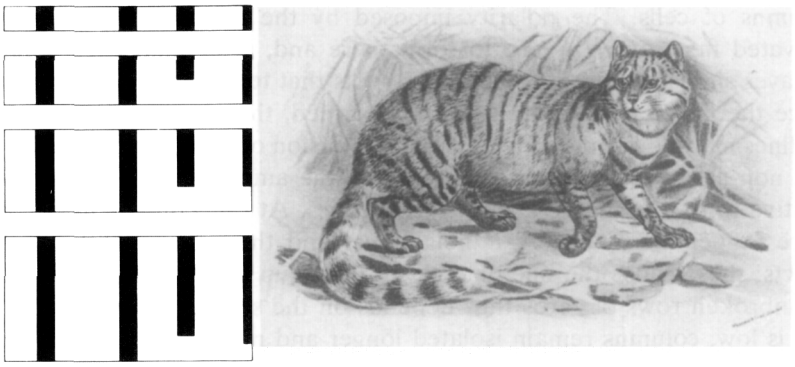

(a) (b)

FIG. 4(a) The emergence of vertical stripes on an array 30 cells wide. The zeros of the Y morphogen are shown in black. The arrays are 3, 6, 9 and 15 cells deep and cells are activated with 5 min delays. In this simulation, the zeros were *not* fixed, $N = 84643$, $S = 0{\cdot}5$, $\sigma = 0{\cdot}05$, $E = 10^{-4}$. (b) The caffre cat, *F. caffra*: in this cat, the most pronunced stripes are dorso-ventral (from Lynnender, 1900).

However, if the first few rows were given 1000 sec before the next cells were activated then the vertical lines started at the top row (Fig. 5a and b). At the molecular level, this difference in time corresponds to the extent to which the kinetics approach equilibrium: if the relative difference between successive interactions were less than 10^{-3} a time of 300 sec was required, if 10^{-4} then 1000 sec. A large difference in times for the kinetics to reach equilibrium is found only in the initial line, after this the time difference in approaching to within 10^{-3} and 10^{-4} of equilibrium is only a few seconds. In other words the difference between the presence and absence of a dorsal stripe here derives from the amount of time available to the system to settle down.

The reason for vertical stripes rather than any other pattern of zeros seems to derive from the strong constraints exerted by an extant pattern on a single, "bland" line of cells. A local "zero" will act as a sink for morphogen Y from an adjacent cell and in the absence of any other constraint will induce that cell itself to become a zero. This property counteracts and in this case dominates the tendency of the chemical kinetics to generate a pattern of spots.

In the biological context, the pattern matches well the flank patterns of the zebras, several members of the *felidae* such as the caffre cat (Fig. 4b– and such *bovidae* as the eland and the kudu; these last animals having thin white stripes on a brown background. The width of the stripe is assumed to derive from the threshold level. Particularly interesting is the fact that

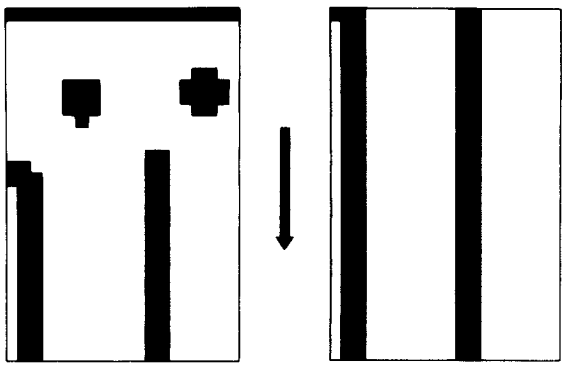

FIG. 5(a) A 20×30 array of cells whose kinetics were initiated by a constant velocity wave moving ventrally at the rate of a cell per 5 min. The zeros of the Y morphogen are shown in black. Computing details: $N = 84643$, $S = 0{\cdot}25$, $\sigma = 0{\cdot}1$, $E = 10^{-3}$, zero-fix option. (b) A simluation identical to that of Fig. 5a except that the velocity of the wavefront was one cell per 1000 sec. This change allowed the kinetics to approach within 10^{-4} of equilibrium before a ventral cell was activated. In fact, after the initial few cells, this criterion was reached within 300 sec.

some animals may have a dorsal stripe while a closely related species may not. For example, the zebras *E. grevyi* and *E. burchelli* tend to have a dorsal stripe whereas *E. zebra* does not. The mechanism shows that a simple difference in the kinetics can explain this morphological difference.

AN EFFECT OF BOUNDARIES ON THE PATTERN

It turns out that the circular boundary conditions that exist on cylindrical arrays can exert a considerable constraint on the pattern (Bard & Lauder, 1974). Provided that the circumference of the cylinder is of similar size to the chemical wavelength, the kinetics generate rings rather than spots. This is best shown on a cone where there are rings at the tip and spots where the circumference increases (Fig. 6a). The reasons for this particular pattern can only be understood in the context of the analytical solutions of the equations (see Murray, 1981). It is worth noting that the circular boundary conditions dominate any other effect: if for example, a constant-velocity wave moves distally down a cone, vertical stripes form initially but, when the cone is narrow, the stripes become circumferential. In the biological context, these simulations suggest that the rings that are seen on the tails of cats (e.g. the serval in Fig. 6b) and on the legs of, say, zebras are generated by reaction–diffusion kinetics constrained by boundary conditions. However, the distance over which the embryo generates rings is

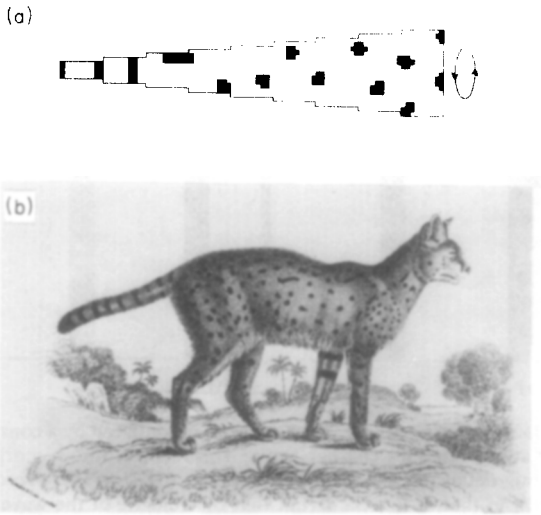

FIG. 6(a) The pattern of Y morphogen zeros that emerged over a cone when all cells were activated simultaneously. Computing details: $N = 84643$, $S = 0{\cdot}5$, $\sigma = 0{\cdot}25$. The pattern emerged within 25 min; zeros not fixed. (b) The serval, *F. serval*: this cat has a pattern of dark spots and rings around the tail. There is also the occasional ring around the legs (from Lynnender, 1900).

probably larger than that over which these kinetics have produced rings. If the chemical wavelength is about 20 or 25 cells, then rings will only form if the circumference is of this size which corresponds to about 500 μm or a diameter of 150 μm. If the wavelength is 50 cells, the largest achieved, the diameter is still only 300 μm. This is small for a limb rudiment but may be within the limits of the early tail. It is therefore premature to accept unequivocally the view that circular boundary conditions are, in general, responsible for generating rings.

Discussion

The results show that reaction-diffusion kinetics can, under appropriate conditions, generate a range of patterns similar to those seen in certain mammals. However, they give no clue as to the extent that this resemblance may, as it were, be only skin deep, reflecting a coincidence rather than giving insight into the biological mechanism. It is quite possible that epidermal differentiation is controlled by some other, as yet unknown, class of mechanisms. The major interest of the work thus lies in knowing whether or not the kinetics provide a "good" model of reality and this is the main point discussed here; the novel and counterintuitive mathematical results

will be examined only in the biological context. Before examining the results in detail, it is worth spending a moment examining the criteria beyond simple simlarity against which the model should be tested. These must include the ability of the kinetics to generate patterns that form within the time and space constraints imposed by the embryo, that are stable to growth and that are capable of explaining not only the normal but also the abnormal patterns that occasionally occur.

It is an unfortunate fact that the only direct evidence that we appear to have on the formation of complex skin patterns in the cats and zebras is what we can observe directly. This is for two major reasons: first, we can't do experiments on the epidermis of early mammalian embryos and, second, it is highly likely that the hair pattern appears a considerable time after the decisions as to which cells should pigment have been taken. Melanoblasts, which derive from the neural crest, reach their final positions at around 3 weeks (the tailbud stage) in the *equidae*. Growth analysis suggests that pigmentation decisions are taken soon after this even though the pigment itself does not appear until about 6 months (see Bard, 1977, for fuller discussion). The analysis does however show that the stripes, when first laid down, are likely to be even having a space of about 0·4 mm (20 cells) and are about 0·5–1·0 mm (25–50 cells) long. The striping process itself probably takes at the most a few days. It is reasonable to suppose that pattern formation in other mammals is not dissimilar.

Turing kinetics can generate patterns within these constraints. Earlier work (Bard & Lauder, 1974) has shown that a chemical wavelength of up to about 50 cells can be achieved by Turing kinetics. The major difference between a pattern of spacing of eight cells and one of 50 cells lies in the time of generation: the period for the kinetics to reach equilibrium depends on the square of the wavelength (simulation times of course also vary as the size of the array). Kinetics giving a wavelength of 20 cells would thus take perhaps six times as long to form as those studied here. The pattern formed by simultaneous activation of cells would take a few hours and that initiated by diffusion perhaps 20–30 hr. In the case of striping initiated by the constant-velocity wave, each cell would require about 50 min to reach equilibrium and, though the wave velocity would have to be less than this, a 50 cell pattern could form within 2 days. Whether or not it is possible for a wavefront to move so slowly remains unclear. It is however no problem in principle for the wavefront to initiate diffusion contact between previously uncoupled cells; the presence of tight junctions that permit such diffusion can be regulated in embryos (e.g. Furshpan & Potter, 1968).

Equally as important as the scale question is that of stability. The *equidae*, at least, appear to grow rapidly during patterning and it is necessary that

any stripes be unaffected by cell division. Note that for stability it is not enough that the pattern be interpreted immediately and irreversibly, as it is possible that all the cells might be switched at one time or another as growth over a day or two caused the concentration contours to move. The original kinetics of Turing were not stable to growth but the zero-fix amendment, whereby once a cell that has no Y maintains this state thereafter, turns out to be acceptably stable. Simulation of this condition on a line of dividing cells, for example, shows that, as the zeros move apart, a new zero eventually forms (see Fig. 7 and its caption for details). In the case of zebra shadow stripes (Fig. 1) which probably arise through growth, there is likely to be some sort of "zero-fix" condition operating irrespective of the details of the mechanism.

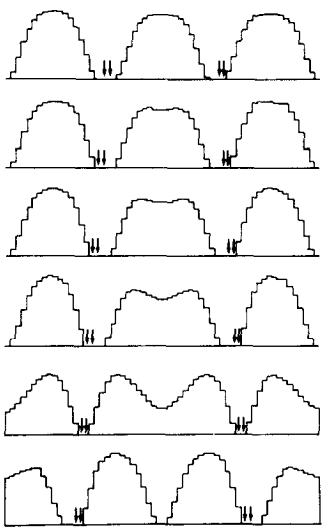

FIG. 7. The equilibrium concentration of the Y morphogen in a line of 60 cells where two pairs of two cells have their zeros fixed (marked by arrows). The maximum concentration is about 7·0 units, the minimum 0·0. Initially, the zeros are 20 cells apart but in successive plots, they are set two further cells apart. It can be seen that at equilibrium ($E = 10^{-3}$) the central peak shows an increasing bifurcation as its width is enlarged.

The major reason for doubting that reaction–diffusion kinetics are responsible for pattern formation *in vivo* is that they have not as yet generated the complete range of unexplained coat patterns. In particular, we have not been able to make vertical stripes bifurcate or join and thus, for example, form the triradius which often occurs where the forelimb buds off from the body. We have also failed in general to simulate conditions which would constrain the kinetics to generate ring contours on cylinders,

the reasonable model for a limb. As yet, it has only proven possible to generate such rings under two sets of conditions: first, when there is diffusion activation of the kinetics over a cylinder, this mechanism is unlikely to operate on a growing limb but could activate a completed one; second, when the kinetics operate over a narrow cylinder whose circumference is similar to that of the wavelength. This last condition is very powerful and the circular boundary conditions dominate any other constraint. It is however limited to tissues whose circumference is <50 cells or whose diameter is perhaps 0·35 mm. This value is smaller than an early limb bud though not, perhaps, the tip of an early tail. What does however seem clear is that the inadequacies of the model occur when the kinetics would have to work over geometries more complex than a simple array. It will therefore be important to study diffusion–reaction kinetics over arrays of cells with more subtle boundary conditions than those considered here.

In this context, it should be noted that Murray (1981) has explored, both analytically and numerically, the ways in which a range of boundaries influence the patterns that emerge with a set of reaction–diffusion kinetics slightly different from that used here. Perhaps his most interesting result is the demonstration that increasing the speed of kinetics over a cone causes the ring pattern to change to one with a dorsal line and D-V stripes, a pattern common in mammals. He also shows that, over an array the shape of a spread skin, increasing the speed causes changes in the gross pattern: a featureless map breaks up successively into two domains, large blotches, small blotches, large blotches and finally again to a virtual absence of pattern. Unfortunately, his computing method, based on finite element techniques does not readily give information on the cellular scale of the pattern nor on the absolute time taken for it to emerge. It is therefore hard to map his results directly onto the embryo. Nevertheless, he does provide important information on the significance of scaling for the formation of melanocyte patterns.

There are some additional features of mammalian coat patterns which further suggest that mechanisms based on reaction–diffusion kinetics are important in controlling melanocyte differentiation. First, there is considerable variation in the biological pattern to the extent that even the two flanks of a single zebra or cat have patterns that clearly differ in detail. In the model system, the stimulus for the kinetics is the existence of small local differences in the molecular concentrations in adjacent cells. As these differences are set up randomly, successive simulations give different but similar patterns (Bard & Lauder, 1974). Unpredictability is thus an intrinsic, necessary part of the model. In the embryo, there will always be unpredictable local differences between cells and it is, at the least, reasonable to

suppose that not only do they have an effect on the pattern details but that the mechanism is stable to them. Second, there are occasional abnormally-patterned zebras: these may be assumed to derive from the striping mechanism degenerating in some way. Before considering them, it is worth noting what would be expected to happen if the model pattern were to break down. As unconstrained Turing kinetics gives spots, it is highly significant that occasional spotted zebras have been reported. I have come across three such animals: the first, *E. burchelli*, had a spotted region on the back, between the neck and the tail extending some 25 cm either side of the dorsal stripe (King, 1965); the second, another example of *E. burchelli*, had over its body rows of white spots rather than stripes (Fig. 8); the third, an *E. burchelli*—horse hybrid (Ewart, 1899; Bard, 1977), had many spots on its rump. These examples provide good evidence that the striping mechanism *in vivo* is at least related to reaction–diffusion kinetics.

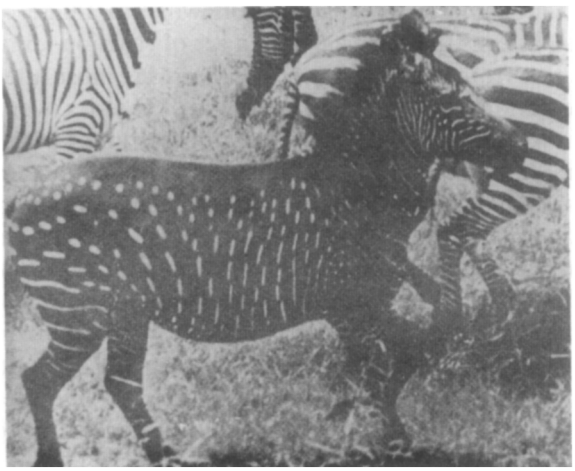

FIG. 8. A rare example of *E. burchelli* with white spots where stripes would be expected (copied from the "Star" newspaper of S. Africa, 30th December 1967).

An interesting highlight on the question of whether zebras are black animals with white stripes or white animals with black stripes is given by this white-spotted zebra (Fig. 8). It is only possible to understand the pattern if the white stripes had failed to form properly and that therefore the "default" colour is black. The role of the striping mechanism is thus to inhibit natural pigment formation rather than to stimulate it. Further evidence for this view comes from the now-extinct *quagga*: this animal is striped on the head and shoulders alone, the unpatterned rump is dark

(Rau, 1974). This analysis does not, however, provide an explanation of the fact that the bellies of *E. zebra* and *E. grevyi* though not *E. burchelli* are usually white; it is possible, however, that this phenomenon has more to do with competence than with striping for there is a white underside on many mammals including tigers, leopards, foxes and antelopes. The conclusion that zebras are black animals with white stripes tallies with the evolutionally-based view of Willoughby (1946) and the opinion of Africans; people of Europe origin tend, on the other hand to assume that the zebra is a white animal with black stripes (c.f. Sanderson, 1955).

The final point that has to be made about the whole model is that it takes a relatively simple view of the embryo as Turing assumed that the cells were identical and their organisation essentially bland, being able only to make and degrade molecules that could diffuse to nearest neighbours. Given current knowledge, this is an oversimplified view: biochemical networks can exist that can cascade and are thus far more complex than those envisaged by Turing and cells may be polarized and anisotropic. It is therefore worth considering what effect in principle these sophistications might have on reaction–diffusion pattern formation. Subtle chemical models have been put forward recently (e.g. Meinhardt & Gierer, 1974; Kaufman, Shymko & Trabert, 1978; Murray, 1981) capable of generating a range of patterns with various regulative abilities but none have, as yet, been shown able to generate the complete range of mammalian pattern elements. I suspect that two-morphogen mechanism alone will not be able to generate patterns that are considerably more complex than those formed by Turing's kinetics. The reason for this belief lies in the fact that it is the marginal reaction rates near an unstable equilibrium point that initiate a pattern. These rate constants have to fit within mathematically-defined limits which are common to all mechanisms. The differences between simple and complex mechanisms lies in the extent of the feed-back and control loops in the kinetics and these modulate rather than initiate patterns. What has yet to be explored is a further and far richer set of kinetics discussed by Turing (1952) which are based on three morphogens and are capable of generating travelling waves; these may be able to form a range of hitherto-unconsidered patterns. Travelling waves have been observed in practice in Zhabotinsky reactions (Zhabotinsky & Zaikin, 1974; Winfree, 1980) which are also capable of generating stripes. It will be interesting to explore experimentally and theoretically what patterns these complex chemical reactions can generate.

The other aspect of the model which is treated very simply here is the cellular array. The patterns that have been generated assumed a formless array with a polarity deriving only from the mode of initiation. It is quite

possible that there exist in tissues before pattern formation polarities that give the cells anisotropic properties so that, for example, diffusion might be faster in a D–V rather than an A–P direction. Such properties may allow simple kinetics to set up patterns more complex than those generated here. The other way that the cellular array could affect the patterns is through the local geometry. It is, for example, clear in the zebras that where the tissue bulges stripes bifurcate and that on legs there are rings. The next stage in exploring theoretical pattern-forming kinetics is to examine the details of these structural aspects.

In conclusion, the approach adopted in this paper views the pattern on mammalian coats as deriving from a combination of reaction–diffusion kinetics, initiation mode, boundary conditions and concentration thresholds for pattern interpretation. The scale of the pattern is determined by the speed of the kinetics relative to diffusion and can be set from three to perhaps 50 cells. While only part of the marking repertoire has so far been generated, it is reasonable to suppose that more of the pattern elements could be generated by using complex geometries and by other modes of initiation—there could well be wavefronts whose properties are intermediate between the decreasing and constant velocities discussed here. Certainly the model provides a temporarily-acceptable paradigm for coat patterns. In the future, better models will be required for the particularly complex patterns that have not been considered here. It is enough to give two examples. The jaguar has on its basically light coat, dark spots surrounded either by a dark ring or a circle of spots. Such a pattern could perhaps be derived from either a cascade process or a very complex interpretation

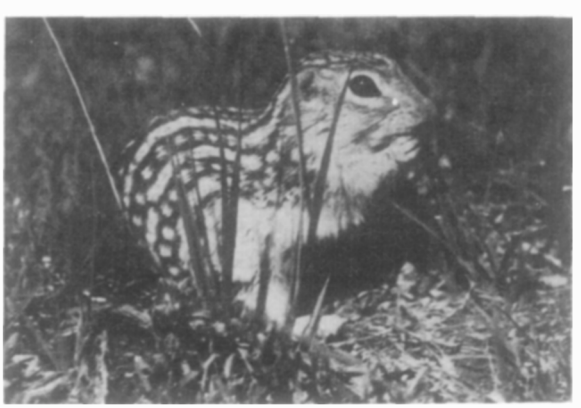

FIG. 9. The thirteen-lined ground squirrel: this pattern cannot be explained, even in principle, by any known mechanism.

system. It is however hard to see how these or any other mechanisms could generate the pattern of the thirteen-lined ground squirrel: this animal, basically brown, has seven *A–P* stripes with six intervening rows of white spots (Fig. 9).

I am most grateful to Ian Lauder for writing the complex computer programs required for this work and I thank Vernon French and Tom Elsdale for commenting on the manuscript.

REFERENCES

BARD, J. B. L. (1977). *J. Zool.* **183,** 527.
BARD, J. B. L. & LAUDER, I. (1974). *J. theor. Biol.* **45,** 501.
BRITTON, N. F. & Murray, J. D. (1979). *J. theor. Biol.* **77,** 317.
EWART, J. C. (1899). *The Pennicuik Experiment.* London: A. and C. Black.
FURCHPAN, E. J. & POTTER, D. D. (1968). *Curr. Topics Develop. Biol.* **3,** 95.
KAUFMAN, S. A., SHYMIK, R. M. & TRABERT, K. (1978). *Science* **199,** 259.
KING, J. M. (1965). *E. Afr. Wild. J.* **3,** 99.
LYNNENDER, R. (1900). *Cats.* London: J. F. Shaw and Co.
LEWIS, J., SLACK, J. M. W. & WOLPERT, L. (1977). *J. theor. Biol.* **65,** 579.
MACWILLIAMS, H. K. & PAPAGERGIOU, S. (1978). *J. theor. Biol.* **72,** 385.
MEINHARDT, H. & GIERER, A. (1974). *J. cell. Sci.* **15,** 321.
MINTZ, B. (1971). *Symp. Soc. Exp. Biol.* **25,** 345.
MURRAY, J. D. (1981). *J. theor. Biol.* **88,** 161.
RAU, R. E. (1974). *Ann. S. Afr. Mus.* **65,** 41.
SANDERSON, I. T. (1955). *Living Mammals.* London: Hamish Hamilton.
SEARLE, A. G. (1968). *Comparative Genetics of Coat Colours in Mammals.* London: Logos Press, Academic Press.
TURING, A. M. (1952). *Phil. Trans. R. Soc.* **237B,** 37.
TWITTY, V. C. (1945). *J. exp. Zool.* **100,** 141.
WILLOUGHBY, D. P. (1946). *Fauna* **83,** 67.
WINFREE, A. T. (1980). *The Geometry of Biological Time.* New York: Springer Verlag.
WOLPERT, L. (1969). *J. theor. Biol.* **25,** 1.
WOLPERT, L. & GINGELL, D. (1970). *J. theor. Biol.* **29,** 147.
ZHABOTINSKY, A. M. & ZAIKIN, A. N. (1974). *J. theor. Biol.* **40,** 45.